A METHOD TO INCREASE THE DEPTH OF FOCUS BY TWO STEP IMAGE PROCESSING

G.HÄUSLER
Optisches Institut der Technischen Universität Berlin, Berlin, Germany

Received 17 July 1972

The method to obtain an increased depth of field consists of two steps. The first step is to produce a modified incoherent image of the three dimensional object which, though degraded, has the same degradation for all object planes. The second step is to filter this modified image in a coherent image processor to obtain un undegraded image with increased depth of focus.

1. Introduction

The higher the aperture of an imaging system the lower is the depth of field. For example in microscopy one obtains a kind of "uncertainty relation"

$$\Delta z(\Delta x^2)^{-1} \leqslant \lambda^{-1} \tag{1}$$

for the depth of field Δz and the resolvable distance Δx. Doubling of resolution means a decrease in the depth of field to the fourth part. That is why especially in high resolution microscopy and high aperture photographic imaging the increase of the depth of focus is of considerable interest.

Two methods especially have been described to overcome the restriction given by (1).

The use of filters in the aperture stop of the imaging system [1] including an annular aperture [2] and the superposition of successively focussed images of different object planes [3–5]. Incoherent filtering has not led to an essential improvement, because the object transfer function (OTF), which is the autocorrelation of the pupil function has its maximum at zero frequency. Therefore one of the tasks, increasing the contrast of higher frequencies, is generally impossible.

Coherent deconvolution of the photograph of a three dimensional object according to Marechal et al. [6] cannot be applied to our problem, because of the different amount of degradation for different image planes.

The pure photographic superposition of successively focussed images results in an improvement of image quality in those parts of the image that would otherwise be defocussed; on the other hand, those parts that would be sharp in a conventional photograph become degraded. By integration along the optical axis in a suitable manner, the complete image though improved in parts suffers from low contrast at high spatial frequencies, similar to the lateral aperture synthesis described by Stroke [7, 8]. To overcome this difficulty we combine incoherent superposition with coherent filtering.

2. Theoretical aspects of incoherent superposition

The first step is to obtain an image with a spread function independent of depth.

The object with depth $2\Delta z$ is moved symmetrically to the plane of sharp imaging by a distance $2z_1$ (see fig. 1). The intensity in the image plane conjugated to $z = 0$ is integrated by a photographic plate. Since telecentric systems are used, the lateral position of an image point is independent of defocussing.

If there are no aberrations, the spread functions of two points positioned symmetrically to the central plane $z = 0$ are equal [9]. The problem is reduced to

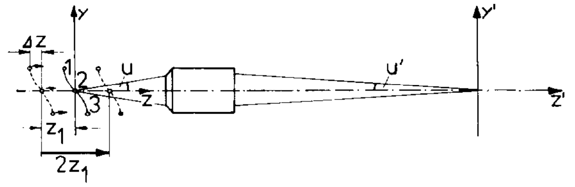

Fig. 1. Principle of incoherent superposition by moving a microscopic object along the optical axis.

the question how to obtain the same spread function for point 1, positioned at the boundary and point 2, positioned in the central plane. This is obviously achieved, when the range of integration $2z_1$ is large in comparison to the depth of the object $2\Delta z$. But because of the limited dynamic range of the photographic plate, too high values of z_1 are disadvantageous. Fortunately it follows from exact calculations that the spread functions are equal in a sufficient approximation if the range of integration is but twice the depth of the object.

The point spread function obtained by integrating along the optical axis is easily estimated by a geometrical approach to have the shape $E(r') \propto 1/r'$, if E is the luminance and r' is the lateral distance to the gaussian image. Consequently the OTF is proportional to the reciprocal spatial frequency. Near the centre of the point spread function where the geometrical approach is not valid diffraction has to be considered.

In order to filter the integrated image, we need the object transfer function of the process described above. Therefore it is suitable not to calculate the point spread function but the OTF by solving the Duffieux integral.

The pupil function $f(s)$ for a defocussed system is according to Hopkins [10]

$$f(s) = \exp(\mathrm{i}\alpha s^2) \tag{2}$$

in the one dimensional case, which is used here to obtain a solution easily to interpret. In (2) s is the normalized spatial frequency, α is the defocussing parameter or the unit of optical depth,

$$\alpha = \tfrac{1}{2} k z' \sin^2 u' = \tfrac{1}{2} k z \sin^2 u \ , \tag{3}$$

u, u' are the aperture angles, z and z' the defocussing distance in the object and image space and $k = 2\pi/\lambda$.

By calculating the autocorrelation of the pupil function we get the OTF for defocussing

$$D(s, \alpha) = (2\alpha s)^{-1} \sin(2\alpha s - \alpha s^2) \ . \tag{4}$$

Calculation of the OTF after integration by moving the object along the optical axis is possible with the assumption of a linear photographic process: while moving the object, more or less degraded point images are linearly superimposed. That means the Fourier transform of the sum of point images is equal to the sum of Fourier transforms of every single point image. As a result of this, the integrated transfer function $\bar{D}$ becomes

$$\bar{D} = N \int_{\alpha_1}^{\alpha_2} D(\alpha)\, \mathrm{d}\alpha \ , \tag{5}$$

with the normalization factor N.

If $\alpha, \alpha_1, \Delta\alpha$ are attached to $z, z_1, \Delta z$ according to (3) and fig. 1 the OTF for the boundary point 1, the point of maximum distance from the imaging system, is

$$\bar{D}_1(s) = \bar{N} \int_{-\alpha_1-\Delta\alpha}^{\alpha_1-\Delta\alpha} (2\alpha s)^{-1} \sin(2\alpha s - \alpha s^2)\, \mathrm{d}\alpha \ . \tag{6}$$

The final result is

$$\bar{D}_1(s) = (4\alpha_1 s)^{-1} \{ \mathrm{Si}[(\alpha_1+\Delta\alpha)(2s-s^2)] + \mathrm{Si}[(\alpha_1-\Delta\alpha)(2s-s^2)] \} \ , \tag{7}$$

where $\mathrm{Si}(t)$ is the sine integral.

For point 2, positioned in the central plane, that means $\Delta\alpha = 0$, it follows from (7)

$$\bar{D}_2(s) = (2\alpha_1 s)^{-1} \mathrm{Si}[\alpha_1(2s-s^2)] \ . \tag{8}$$

Since

$$\lim_{t\to\infty} \mathrm{Si}(t) = \pi/2 \ , \tag{9}$$

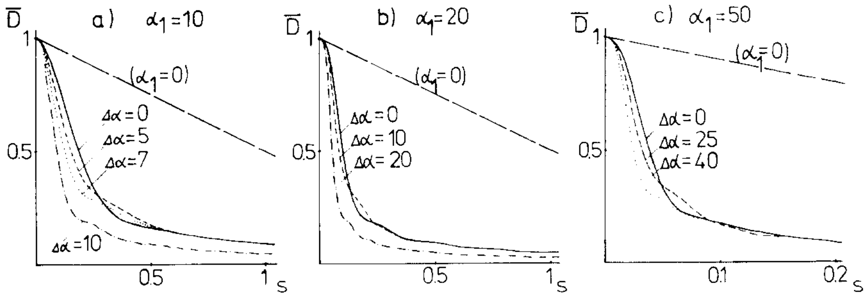

Fig. 2. Integrated transfer function $\bar{D}(s)$ for different ranges of integration $2\alpha_1$ and different depths of the object $2\Delta\alpha$. (Changed scale of abscissa in fig. 2c.)

it follows from (8)

$$\lim_{\alpha_1(2s-s^2)\to\infty} \bar{D}_2(s) \propto 1/s\ , \qquad (10)$$

which confirms the result of the geometrical approach.

Because of the analytical representation of the solution, numerical calculation is easily done on a small computer. In figs. 2a, b, c, $\bar{D}(s)$ is plotted for different ranges of integration and different depths of the object. The difference between the transfer functions $\bar{D}_1$ and $\bar{D}_2$ is negligible if the depth of the object is about half the range of integration. This is an important result for practical use, since the lower the required range of integration, the higher the signal to noise ratio that can be obtained.

The integrated transfer function has no negative values in contrast to defocussing. Therefore the integrated photograph already shows more details (see fig. 3b). Furthermore the deconvolution filter is easy to make.

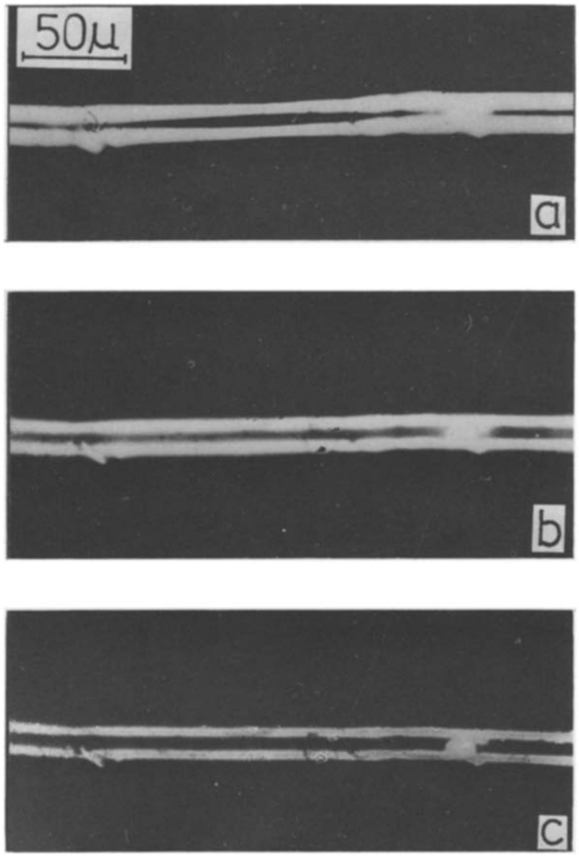

Fig. 3. (a) Conventional microphotograph of a double slit, depth of the object ± 5μ, numerical aperture 1.32. According to (3) this depth is equivalent to $\Delta\alpha$ = 50. (b) Integrated microphotograph (range of integration ± 10μ). (c) After coherent filtering of (b).

3. Experimental results

The integrated photograph was filtered in a conventional coherent image processor. The transparency of the deconvolution filter was indirectly proportional to the transfer function $\bar{D}$. Some results of preliminary experiments are shown in figs. 3, 4 and 5.

In figs. 3 and 4 the range of integration is, according to the calculations, twice the depth of the object, to obtain the same OTF for every image point. The object in fig. 5 consists essentially of dark lines on light ground. That is why the resulting integrated image suffers from very low contrast, which can be

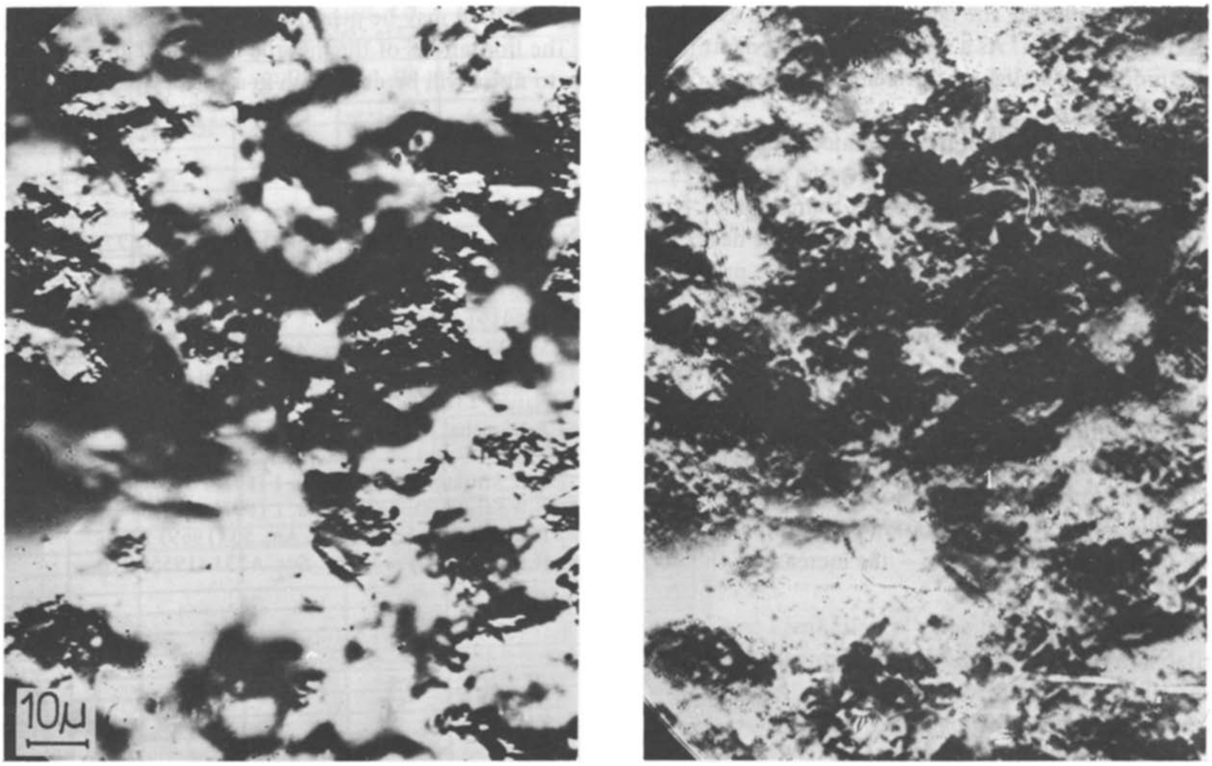

(a) (b)

Fig. 4. (a) Conventional microphotograph of a ground glass with obliquely evaporated thin aluminium layer. Depth of the object $\pm 5\mu$, numerical aperture 1.32. (b) After integration (range of integration $\pm 10\mu$) and coherent filtering.

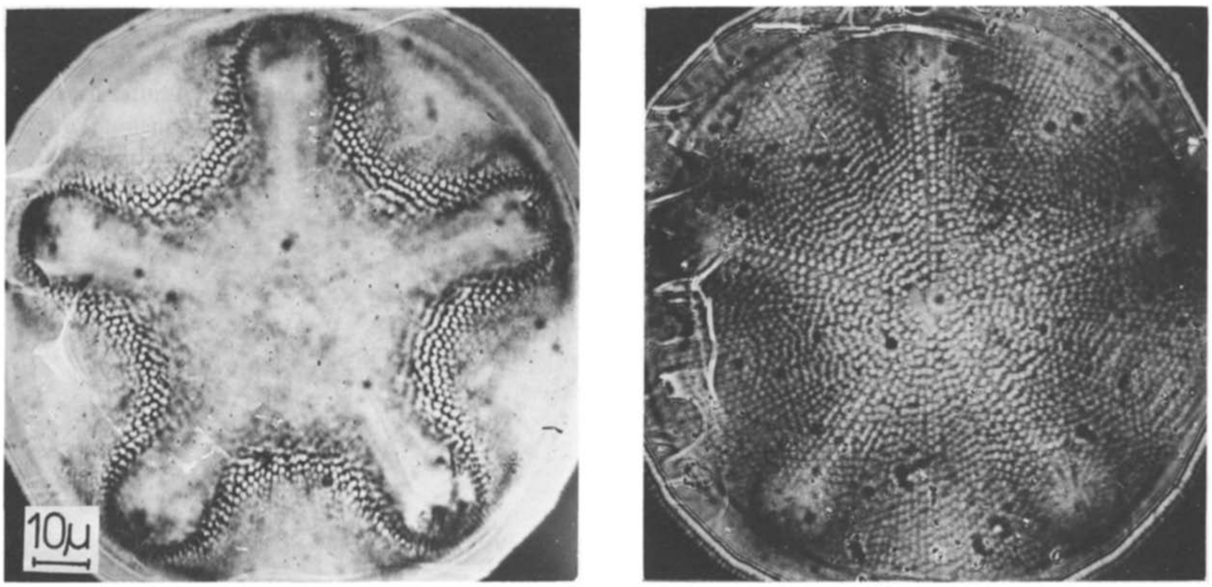

(a) (b)

Fig. 5. (a) Conventional microphotograph of a diatomic. Depth of the object $\pm 8\mu$, numerical aperture 1.32. (b) After integration (range of integration $\pm 10\mu$) and coherent filtering.

increased by reducing the range of integration as done here from 16 to 10μ. As a result the improvement by image processing is slightly different for different object planes (see fig. 5b).

The lack of contrast in the integrated image can be compensated for by a kind of prefiltering with high γ photographic emulsion. But in order to make the method suitable for practical use, it would be desirable to replace the complicated photographic process by a real time method.

Until now photochromic materials do not seem to qualify for this task. On the other hand television systems are gradually used more and more for quantitative picture analysis. Because of the simplicity of the OTF the electronic realization of the deconvolution filter is easy. So with electronic filtering of the integrated image – the integration for example can be done on a luminescent screen – the increase of the depth of field may be possible in a real time process.

The limitations of the method described above due to noise will be dealt with in a further paper.

References

[1] M.Mino and Y.Okano, Appl. Opt. 10 (1971) 2219.
[2] T.Welford, J. Opt. Soc. Am. 50 (1960) 749.
[3] L.Bergmann and G.H.Becker, Deutsche Patentschrift 1029591 (1958).
[4] M.C.King and D.H.Berry, Appl. Opt. 10 (1971) 208.
[5] J.F.Burke, G.Indebtouw, G.Nomarski and G.W.Stroke, Nature 231 (1971) 303.
[6] A Maréchal, P.Croce and K.Dietzel, Opt. Acta 5 (1958) 256.
[7] G.W.Stroke, Opt. Commun. 1 (1970) 283.
[8] G.W.Stroke, Opt. Commun. 1 (1970) 287.
[9] P.A.Stokseth, J. Opt. Soc. Am. 50 (1969) 1314.
[10] H.H.Hopkins, Proc. Roy. Soc. A231 (1955) 91.